

NOTES AND CORRESPONDENCE

Transient Response of an Atmospheric GCM to North Atlantic SST Anomalies

Z. X. LI AND S. CONIL

Laboratoire de Météorologie Dynamique, CNRS, Paris, France

9 September 2002 and 23 May 2003

ABSTRACT

A high-resolution atmospheric general circulation model (GCM) is used to evaluate the atmospheric response to North Atlantic sea surface temperature (SST) anomalies. The transient evolution of the response is studied in detail. The linear and nonlinear effects can thus be contrasted and separated by their different time scales. Baroclinic patterns related directly to the surface anomalies quickly reach their maximum manifestation. However, barotropic patterns related to the mid- and upper troposphere eddy vorticity fluxes have longer time scales with much more important amplitude, able to gradually replace the initial baroclinic response. This study thus provides an evolutionary picture of the two types of response in a GCM.

1. Introduction

It is generally agreed that the extratropical sea surface temperature (SST) anomalies are essentially created by variations in surface radiative, sensible, and latent heat fluxes and wind-induced Ekman currents. It is also expected that the ocean, due to its large dynamical and thermal inertia, can provide useful boundary conditions for climate prediction through the SST anomalies. How do the extratropical SST anomalies exert their influence on atmospheric variability and thus be used for short- and medium-range climate prediction? This question is a natural extension of the successful climate prediction studies based on tropical SST anomalies (El Niño, in particular). However, the answer to this question is much more difficult, because the atmospheric response to extratropical SST anomalies is weak and the atmospheric internal variability is large (low signal-to-noise ratio).

The first consideration of the response was provided through the quasigeostrophic theory that is relevant to the extratropics (Hoskins and Karoly 1981; see Frankignoul 1985 for a review): a surface heating is equivalent to a source of potential vorticity at the lower boundary, with a compensating sink above. This creates a baroclinic response in which the surface heating (cooling) initiates a low-level low pressure (high pressure) and a high-level high pressure (low pressure), similar to the midlatitude atmospheric patterns related to the seasonal variation of the land–sea contrast.

The midlatitude atmosphere has a strong component of transient circulation and can reveal a large nonlinear response to SST anomalies through changes of statistical properties of the atmospheric eddies (amplitude and shape of individual events, frequency of their occurrence, and geographic location of their path). An equivalent barotropic response can be excited through changes on upper-tropospheric eddy-induced vorticity and perturbation of the associated storm tracks. The exact final response, unlike the above-mentioned baroclinic response, can no more be obtained through a simple intellectual deduction. This is similar to the extratropical response to tropical SST anomalies (Lau and Nath 1996).

In the last two decades, many authors have used general circulation models (GCMs) to seek the atmospheric response to midlatitude SST anomalies (see the review paper of Kushnir et al. 2002). Results, from baroclinic patterns (Kushnir and Held 1996) to equivalent barotropic ones (Peng et al. 1997; Ferranti et al. 1994), are often nonconclusive and sometimes contradictory. Recent studies using improved physical parameterizations, higher model resolution, and larger ensemble size seem to reveal that the important factors determining the response are the basic climatological state, intensity of the transient circulation, and its feedback on the large-scale flow.

An important study in reconciling the linear and nonlinear effects and in revealing the role of the transient eddies was reported in Ting and Peng (1995) and in Peng and Whitaker (1999). The transient eddy forcing resulting from a midlatitude SST anomaly was diag-

Corresponding author address: Laurent Z.X. Li, LMD, casier 99, Université Paris 6, 4, place Jussieu, 75252 Paris cedex 05, France.
E-mail: li@lmd.jussieu.fr

nosed from full GCM calculations and then used to force a linear model, in the same manner as for internal variability or the response to tropical forcing. Results clearly explained the difference between the full GCM response and the direct linear response to heating. In particular, the response to transient eddy vorticity fluxes was able to reverse the linear near-surface effect, replacing a baroclinic structure by an equivalent barotropic one.

The present study aims also to reconcile the linear and nonlinear effects of midlatitude SST anomalies. The main hypothesis to explore is that the linear and nonlinear effects should have different time scales of manifestation. We can thus differentiate between them by analyzing the time evolution of the response and the manner by which the equilibrium is reached.

2. Model and experiments

The model used is LMDZ, the atmospheric general circulation model developed at the Laboratoire de Météorologie Dynamique (LMD). It is derived from the standard LMD model described in Sadourny and Laval (1984). A brief description of the LMDZ's physical parameterization and climate performance can be found in Li (1999). To ensure a good representation of the model's transient circulation, a high-resolution version is employed with 150 points in latitude and 200 in longitude. There are 19 vertical levels. To further increase the model resolution in the region of our interest (North Atlantic and Europe), a local zoom is applied with the center located at 45°N, 5°E (French Rhone Valley). The model resolution is about 60 km near the center of the zoom and decreases progressively (according to a sinusoidal function) away from the center to about 240 km near New Zealand, in the Southern Hemisphere. The same model version was already used in Zhou and Li (2002) to study the Asian summer monsoon, the zoom center being put, in that case, over China.

A first experiment has been conducted in a seasonal mode for 10 yr of simulated time. It includes a control simulation and a perturbed one. The control was forced by seasonally varied climatological boundary conditions: SST and sea ice extension averaged for the period 1979–95. The perturbed simulation is identical to the control, but SST anomalies were added in the North Atlantic corresponding to the dominant structure in this region, as described in Rodwell et al. (1999). Figure 1 shows the geographical distribution of the SST anomalies. Both of the two simulations were run for 10 yr, but only the averaged January situations will be shown. This experiment will be considered as equilibrium results.

The second experiment has been conducted in a perpetual January mode. The model was run for a length of 8 days for both climatological boundary conditions and above-given SST anomalies. To surpass the obstacle related to the chaotic behavior of the atmosphere and

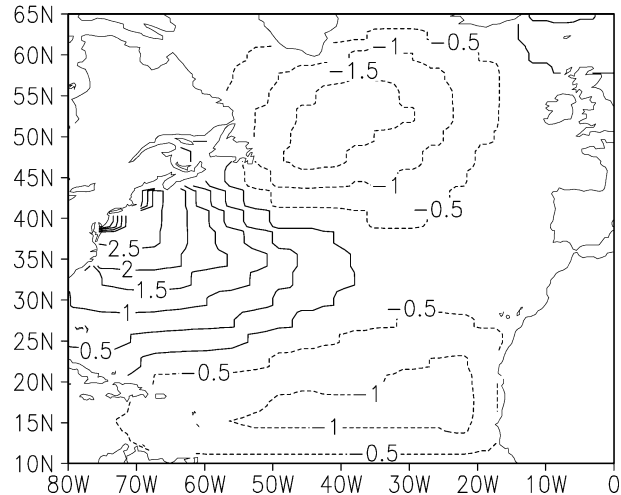


FIG. 1. Dominant structure of the North Atlantic SST anomalies used to force the AGCM. The amplitude is scaled to have twice the observed typical variations (Rodwell et al. 1999).

to ensure a good representation of the January climatology, the ensemble approach was used with different initial conditions, in a similar manner as employed by a weather prediction center for its ensemble prediction system. The size of our ensemble is 240 and the ensemble averages (two meteorological sequences of 8 days) will be inspected to study the transient response of the GCM.

3. Results

Figure 2 displays the geopotential height anomalies for, from top to bottom, 200, 500, 700, 850, and 1000 hPa, respectively. The time evolution is revealed by different columns from left to right, corresponding, respectively, to days 1, 2, 4, and 8 of the second experiment. The last column is the equilibrium situation (first experiment), showing clearly an equivalent barotropic response for almost the whole domain. The most noticeable structure is the North Atlantic Oscillation (NAO) characterized by a low pressure center situated between the British Isles and Iceland, and a high pressure center that occupies the main part of the North Atlantic basin. Compared to the observed NAO, which has a strong relationship with the tripolar SST anomalies (see, e.g., Czaja and Frankignoul 2002), the NAO structure in our model is slightly shifted to the south. This is the consequence of a bias in our model (also very common in other currently used general circulation models), that is, the simulated planetary waves are a bit weak in the North Atlantic sector. The intrinsic internal variability thus presents a southward-shifted structure, and so does the atmospheric response to the SST anomalies with its strong projection onto the internal variability structure (Peng and Robinson 2001; Peng et al. 2002). In the south part of the domain, a baroclinic

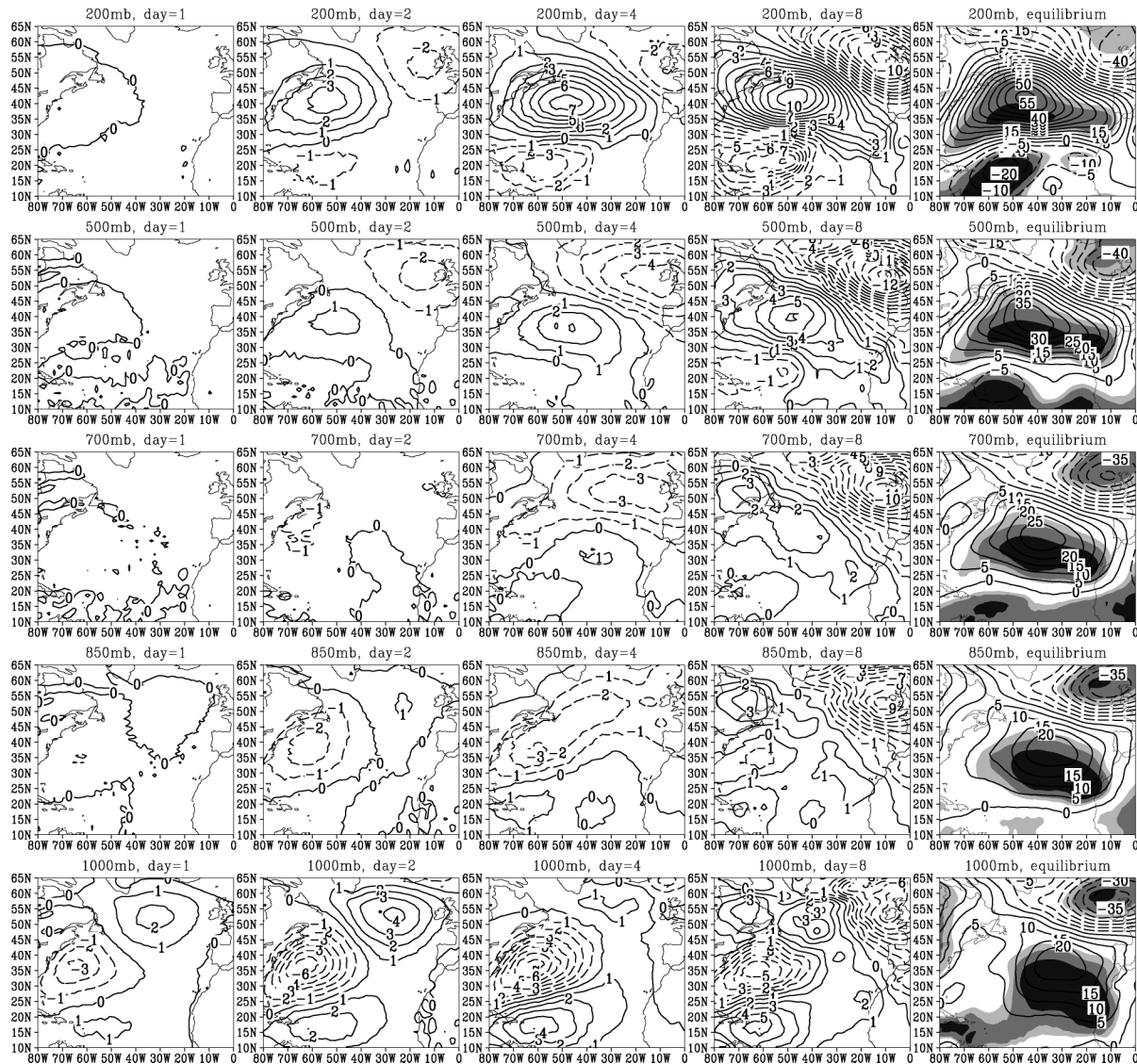


FIG. 2. Geopotential height anomalies for different levels of the atmosphere (rows) and at different times (columns). (top to bottom) The anomalies are plotted at 200, 500, 700, 850, and 1000 hPa, respectively. (left to right) The time evolutions are plotted for days 1, 2, 4, and 8, respectively. The last column gives the corresponding anomalies at equilibrium. Contour interval is 1 m, except for the last column where it is 5 m. Statistical significance at 60%, 75%, and 90%, calculated through a simple point-to-point t test, is shaded for the last column.

structure is visible, since a low at mid- and upper levels accompanies a weak high near the surface.

The second column from the right in Fig. 2 is the situation for the eighth day of the transient experiment. The main spatial features of the equilibrium experiment are very well established, especially above 700 hPa. The amplitude for day 8 in the transient experiment, however, is much smaller than the equilibrium experiment. A factor of 3–6 is generally observed. This may indicate that a complete establishment of the equivalent barotropic response is beyond the synoptic scale and extends likely to monthly or even longer time scales. The short time sequence in this study does not allow a precise evaluation of the needed adjustment time. This adjust-

ment time certainly has a large theoretical interest for understanding the atmospheric low-frequency variability, but in the real atmosphere, we need also to consider the interaction with the seasonal cycle.

Let us now examine the time evolution in the transient experiment. At the beginning of the sequence, a tripole structure is visible near the surface, corresponding to the direct effect of the SST anomalies. The baroclinic structure is very clear for day 2, because patterns of opposite sign are observed above and below 700 hPa. After day 2, the 200-hPa situation keeps a similar structure, but its amplitude continues to grow. For the northern part of the domain, the 200-hPa anomalies propagate downward and progressively entrains the whole atmo-

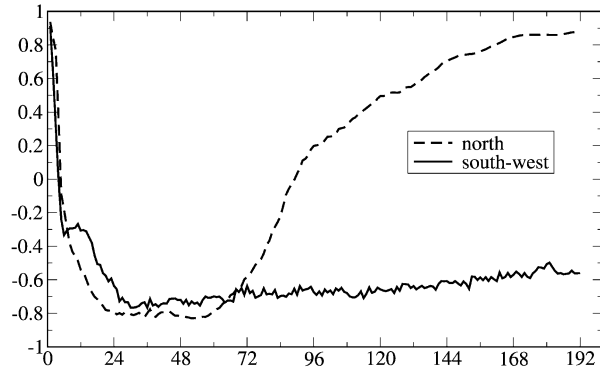


FIG. 3. Spatial correlation coefficients as a function of time (hours, labeled with daily interval) measuring the horizontal pattern resemblance between the geopotential height anomalies at 200 and those at 850 hPa. Positive correlation indicates vertical barotropic structure and negative correlation indicates baroclinic structure. The dashed curve is for the subdomain north of 30°N and the solid curve is for the southwest corner of the domain shown in Fig. 1, i.e., south of 30°N and west of 40°W .

sphere toward an equivalent barotropic structure. The southwest corner of the domain remains in a strong baroclinic structure even in the end of the 8-day sequence.

To quantify the above-described barotropic and baroclinic character, we evaluate the spatial pattern resemblance between the high (200 hPa) and low (850 hPa)

levels of the atmosphere. To do so, we calculate the spatial correlation coefficient and show, in Fig. 3, its evolution in time. The calculation has been done for, respectively, the south ($10^{\circ}\text{--}30^{\circ}\text{N}$, $80^{\circ}\text{--}40^{\circ}\text{W}$) and north ($30^{\circ}\text{--}65^{\circ}\text{N}$, $80^{\circ}\text{W--}0^{\circ}$) subdomains. Both curves in Fig. 3 show a rapid evolution to negative values, revealing a quick establishment of the baroclinic structure that is coherent with the linear response theory. The southern part remains baroclinic (negative correlation) all the time, but the curve of the northern part goes up to positive correlations from around 96 h (4 days) and becomes strongly barotropic at the end of the 8-day sequence.

Vertical structure of the atmospheric response and its time evolution can also be revealed in Fig. 4, showing geopotential height anomalies in sections following longitudes 60° , 30° , and 10°W . As mentioned before, we can observe a strong baroclinic structure around day 2, showing the direct linear effect of the SST anomalies. The barotropic response is then progressively installed through an intensification of the mid- and high-level responses and a replacement of the low-level structures by the high-level ones. This adjustment is achieved faster in the eastern basin than in the western basin: the barotropic structure is already well established at day 4 for the section at 10°W , but a strong baroclinic character remains at 60°W , even at the end of the transient experiment. This is particularly true for the southern part.

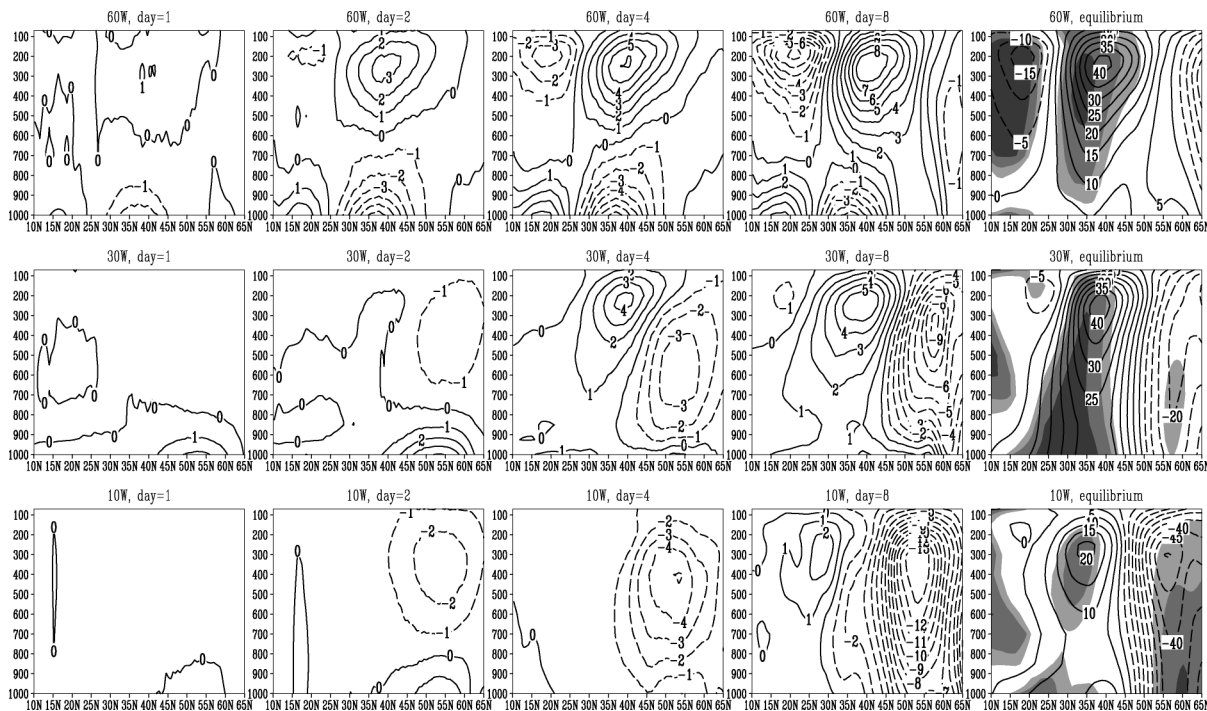


FIG. 4. Latitude–height sections showing geopotential height anomalies at (top row) 60° , (middle row) 30° , and (bottom row) 10°W , respectively. (left to right) Columns indicate time evolution for days 1, 2, 4, and 8, respectively. The last column is for the equilibrium. Contour interval is 1 m, except for the last column where it is 5 m. Statistical significance at 60%, 75%, and 90%, calculated through a simple point-to-point t test, is shaded for the last column.

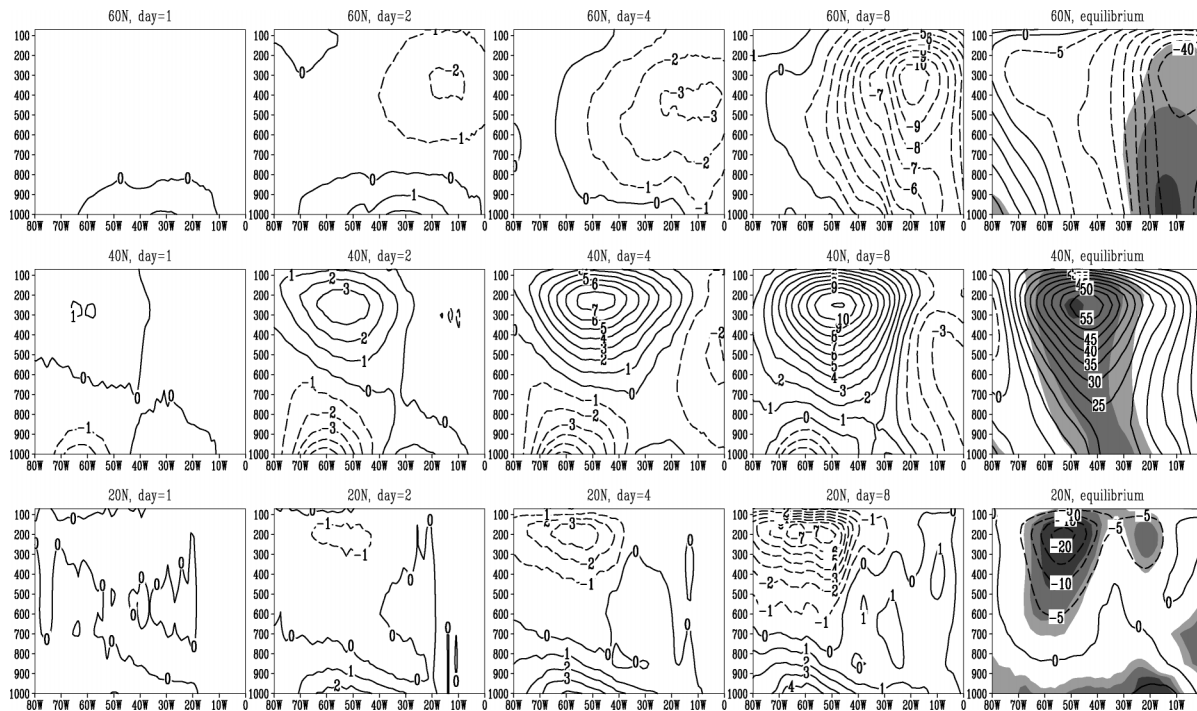


FIG. 5. Same as in Fig. 4, but for longitude–height sections at (top row) 60° , (middle row) 40° , and (bottom row) 20° N.

Figure 5 shows geopotential height anomalies in vertical sections following latitudes 60° , 40° , and 20° N. The transition from the baroclinic to the barotropic structure is faster in the northern part than in the southern part. Considering the fact that the transient circulation of the atmosphere is much more important in the north than in the south, it is then easier to understand why the barotropic response, related to the transient eddy activities, is achieved faster in the northern part. The 20° N section remains baroclinic at the end of the transient experiment, even in the equilibrium simulation. This region is under strong subsidence area where transient circulation is weak and the direct linear thermal heating effect is thus strongly manifested.

4. Conclusions

With a high-resolution state-of-the-art atmospheric GCM, we have investigated the impact of the North Atlantic SST anomalies (in the tripolar form) on the atmospheric circulation. The model was first run for 10 yr to study the equilibrium response. A NAO-type structure is obtained in the North Atlantic basin for January: a low between the British Isles and Iceland and a high in the south and west. The response is equivalent barotropic, with anomalies of the same sign for the whole troposphere. This result is coherent with those of Rodwell et al. (1999) and Mehta et al. (2000) showing that a tripolar pattern of SST anomalies could exert a forcing for the North Atlantic Oscillation and its potential predictability.

To understand the mechanism controlling this response, we designed a second experiment to inspect the dynamical evolution of the response by running the model for an 8-day meteorological sequence. The ensemble approach was employed to minimize the chaotic character of the atmosphere and to ensure a good representation. It is the first time that a baroclinic response and an equivalent barotropic response were both produced in a GCM.

The baroclinic response is a direct effect of the SST anomalies and a linear response of the atmosphere in a hydrostatic and geostrophic manner. This response is almost independent of time and basic state. It reaches its maximum manifestation after two days, the time necessary for the surface anomalies to penetrate into the atmosphere. It would continue to grow until a new equilibrium was reached with the changed heating, but it is increasingly masked by the equivalent barotropic response.

The equivalent barotropic response is first achieved in the upper layers of the atmosphere, and then propagated downward to the whole column. Our results are coherent with theories based on upper-tropospheric transient eddy vorticity fluxes (Peng and Whitaker 1999; Hall et al. 2001). This nonlinear equivalent barotropic response is in general much stronger than the linear baroclinic response. It is time dependent and the time scale of its action varies in function of the eddy activities. In the northern part of the North Atlantic where the transient circulation is intense, the equivalent barotropic response is achieved quickly. It takes a longer

time, however, in the southern part of the basin. For the subtropical region, the equivalent barotropic response is very weak, because the mean circulation is the dominant one. The linear response is still visible even after the equilibrium.

Our results may also have implication for studies on mid- and high-latitude ocean–atmosphere interactions by providing clear evidence that multiple time scales exist for atmospheric response to oceanic anomalies, from an almost immediate linear baroclinic response (one to two days) to an intraseasonal (several tens of days) nonlinear equivalent barotropic response. One needs to incorporate this concept into any considerations regarding ocean–atmosphere coupling.

Finally, we should point out that our results need to be confirmed in other models with longer simulations and larger ensemble sizes. In fact, the equilibrium simulation of 10 yr seems to be too short to get a good statistical significance and the ensemble size (240) of the transient experiment might also be too small.

Acknowledgments. This work is supported by the national French programs PNEDC and GICC. Computer resources were allocated by IDRIS, the computer center of the CNRS. Figure 3 was prepared with the help of Ms. Jennyfer Miot. Stimulating discussions with F. D’Andrea, C. Frankignoul, and F. Lott are acknowledged. The authors also thank W. Robinson and two anonymous reviewers for their useful and encouraging comments.

REFERENCES

- Czaja, A., and C. Frankignoul, 2002: Observed impact of Atlantic SST anomalies on the North Atlantic Oscillation. *J. Climate*, **15**, 606–623.
- Ferranti, L., F. Molteni, and T. N. Palmer, 1994: Impact of localized tropical and extratropical SST anomalies in ensembles of seasonal GCM integrations. *Quart. J. Roy. Meteor. Soc.*, **120**, 1613–1645.
- Frankignoul, C., 1985: Sea surface temperature anomalies, planetary waves and air–sea feedback in the middle latitudes. *Rev. Geophys.*, **23**, 357–390.
- Hall, N. M. J., J. Derome, and H. Lin, 2001: The extratropical signal generated by a midlatitude SST anomaly. Part I: Sensitivity at equilibrium. *J. Climate*, **14**, 2035–2053.
- Hoskins, B. J., and D. J. Karoly, 1981: The steady linear response of a spherical atmosphere to thermal and orographic forcing. *J. Atmos. Sci.*, **38**, 1179–1196.
- Kushnir, Y., and I. M. Held, 1996: Equilibrium atmospheric response to North Atlantic SST anomalies. *J. Climate*, **9**, 1208–1220.
- , W. A. Robinson, I. Bladé, N. M. J. Hall, S. Peng, and R. Sutton, 2002: Atmospheric GCM response to extratropical SST anomalies: Synthesis and evaluation. *J. Climate*, **15**, 2233–2256.
- Lau, N. C., and M. J. Nath, 1996: The role of the atmospheric bridge in linking tropical Pacific ENSO events to extratropical SST anomalies. *J. Climate*, **9**, 2036–2057.
- Li, Z. X., 1999: Ensemble atmospheric GCM simulation of climate interannual variability from 1979 to 1994. *J. Climate*, **12**, 986–1001.
- Mehta, V. M., M. J. Suarez, J. V. Manganello, and T. L. Delworth, 2000: Oceanic influence on the North Atlantic Oscillation and associated Northern Hemisphere climate variations: 1959–1993. *Geophys. Res. Lett.*, **27**, 121–124.
- Peng, S., and J. S. Whitaker, 1999: Mechanisms determining the atmospheric response to midlatitude SST anomalies. *J. Climate*, **12**, 1393–1408.
- , and W. A. Robinson, 2001: Relationships between atmospheric internal variability and the responses to an extratropical SST anomaly. *J. Climate*, **14**, 2943–2959.
- , —, and M. P. Hoerling, 1997: The modeled atmospheric response to midlatitude SST anomalies and its dependence on background circulation states. *J. Climate*, **10**, 971–987.
- , —, and S. Li, 2002: North Atlantic SST forcing of the NAO and relationships with intrinsic hemispheric variability. *Geophys. Res. Lett.*, **29**, 1276, doi:10.1029/2001GL014043.
- Rodwell, M. J., D. P. Rowell, and C. K. Folland, 1999: Oceanic forcing of the wintertime North Atlantic Oscillation and European climate. *Nature*, **398**, 320–323.
- Sadourny, R., and K. Laval, 1984: January and July performance of the LMD general circulation model. *New Perspectives in Climate Modelling*, A. Berger and C. Nicolis, Eds., Elsevier, 173–198.
- Ting, M., and S. Peng, 1995: Dynamics of early and middle winter atmospheric responses to northwest Atlantic SST anomalies. *J. Climate*, **8**, 2239–2254.
- Zhou, T. J., and Z. X. Li, 2002: Simulation of the East Asian summer monsoon using a variable resolution atmospheric GCM. *Climate Dyn.*, **19**, 167–180.